Adsorption of methylene blue onto activated carbon obtained from ZnCl2

Article *in* Desalination and Water Treatment · January 2017

DOI: 10.5004/dwt.2017.0172

3 authors:

Sait Yorgun
Eskisehir Osmangazi University
20 PUBLICATIONS **1,461** CITATIONS

SEE PROFILE

Naile Karakehya
Eskisehir Osmangazi University
16 PUBLICATIONS **337** CITATIONS

SEE PROFILE

Derya yıldız
Eskisehir Osmangazi University
15 PUBLICATIONS **495** CITATIONS

SEE PROFILE

Desalination and Water Treatment
www.deswater.com

doi: 10.5004/dwt.2017.0172

58 (2017) 274–284
January

Adsorption of methylene blue onto activated carbon obtained from $ZnCl_2$ activation of paulownia wood: kinetic and equilibrium studies

Sait Yorgun*[,a], Naile Karakehya[b], Derya Yıldız[a]

[a]*Department of Chemical Engineering, Engineering and Architecture Faculty, Eskişehir Osmangazi University, 26480 Eskişehir, Turkey, Tel. +90 222 2393750/3666; Fax: +90 222 2393613; email: syorgun@ogu.edu.tr (S. Yorgun), Tel. +90 222 2393750/3653; email: dozcan@ogu.edu.tr (D. Yıldız)*

[b]*Environmental Control and Protection Programme, Eskişehir Vocational School, Eskişehir Osmangazi University, 26480 Eskişehir, Turkey, Tel. +90 222 2361415/4519; Fax: +90 222 2361444, email: nkarakehya@ogu.edu.tr (N. Karakehya)*

Received 8 February 2016; Accepted 1 June 2016

ABSTRACT

In this study, an activated carbon was prepared from paulownia (*P. tomentose*) wood by chemical activation with $ZnCl_2$. Pore properties including surface area, pore volume, pore size distribution and average pore diameter of the activated carbon were determined by N_2 adsorption at 77 K using the BET, *t*-plot and density functional theory (DFT) methods. The activated carbon had a BET surface area of 2736 $m^2\ g^{-1}$ and total pore volume of 1.387 $cm^3\ g^{-1}$. The use of activated carbon for the removal of methylene blue (MB) from aqueous solutions was investigated in a batch system different pH, initial dye concentrations contact times, temperatures and adsorbent doses. The extent of dye removal decreased with increasing initial MB concentration and increased with increasing contact time, temperature and adsorbent dosage. The equilibrium data were analyzed by the Langmuir and Freundlich isotherm models. The experimental data for the adsorption of MB dye fit the Langmuir isotherm model very well and the maximum monolayer adsorption capacity of the activated carbon was determined as 322.58, 384.61, 370.37 mg g^{-1} for 25, 35 and 45°C, respectively. The adsorption kinetics were found to follow a pseudo-second-order kinetic model. The changes in entropy (ΔS°) and heat of adsorption (ΔH°) for MB adsorption on activated carbon were positive.

Keywords: Paulownia wood; Activated carbon; Methylene blue; Adsorption kinetics; Isotherms; Thermodynamics

1. Introduction

Demand for different raw materials, water and energy is increasing continuously all over the world due to industrial development, urbanization and pollution growth. Pollution from various industries and from burning fossil fuels results in significant environmental problems including contamination of soil, water and air. Consequently, environmental pollution has become a significant challenge to human beings [1]. Environmental regulations have forced industries to reduce and/or eliminate wastes. Therefore, industry has adapted to adopt sustainable development approaches. Growing concerns about the environment have resulted in the development of new environmental technologies, materials, and ways to reduce and minimize wastes [2]. Waste control, recycling and reuse are very important and increasingly common. Synthetic dyestuffs are among various pollutants that affect waters. They have been increasingly used in many industries, including printing and dyeing, the food industry, and the production of textiles, carpet, leather, tanning, paper, printing, rubber, plastics, cosmetics, and pharmaceuticals, among others [3, 4]. Synthetic dyes have complex aromatic molecular structures that provide

* Corresponding author.

physico-chemical, thermal and optical stability [5]. Dyes are inert and difficult to bio-degrade when discharged into waste streams [6]. Some dyes are mutagenic and/or carcinogenic due to the presence of metal ions and other chemicals in their structures. These dyes are generally toxic: They consume the oxygen dissolved in water, and thus negatively affect aquatic life. Therefore, dyes in industrial effluents are considered to be potential sources of water pollution and pose serious threats to the environment [7]. Several methods are available for the removal of colors, odors, organic and inorganic matter from chemical processes or waste effluents, including membrane separation, aerobic and anaerobic degradation using various microorganisms, chemical oxidation, coagulation and flocculation, reverse osmosis and solvent extraction [8–10]. However, these techniques have disadvantages of incomplete removal, high cost or side effects such as producing additional wastes [11]. Among the advanced chemical or physical treatments, adsorption is considered to be more effective, more convenient, less expensive and easier to operate than other technologies [8, 10–15]. The removal of colored and colorless organic pollutants from industrial wastewater is an important application of an adsorption process [14–15]. The nature of the precursor, activation method, and activation conditions determine the characteristics of porosity in activated carbon, including pore size distribution, pore shape, and surface chemistry [16–20]. Chemical activations are widely used to generate activated carbon from carbon-containing materials. In chemical activation, the carbonization and the activation step occur simultaneously [9, 20–22].

Major advantages of chemical activation are higher activated carbon yield, lower temperature of activation (i.e., lower energy cost), less activation time and, generally, higher development of porosity. The use of biomass as a precursor for producing activated carbon results in some advantages over using coal [23]. Biomass is renewable and widely available in large quantities. It is inexpensive and environmentally friendly, and it has high carbon and low ash contents. The high concentration of volatiles associated with biomass is ideal for creating highly porous structures within the activated matrix [24, 25]. Utilization of forestry wastes as raw material for the production of activated carbons has increased notably in recent years. There are many studies in the literature relating to preparation and characterization of activated carbon from various wood and forest wastes [18, 20, 22, 23, 26–32].

Paulownia is an economically important genus in the family Scrophulariaceae, comprising nine species of very adaptable and fast-growing timber tress. It can be harvested for wood in 4 to –7 years [33]. Paulownia trees have a high biomass production and re-sprouting potential; up to 50 t ha^{-1} y^{-1} [34]. Paulownia is receiving increasing attention as a genus suitable for use as a short-rotation wood crop in many parts of the world [20, 35]. Paulownia plants have been used to produce leaves useful as fodder or fertilizer, flowers for medicine or honey production, wood for solid products, and pulp to produce fine paper and activated carbon [20, 33–35]. There is only very limited study in the existing literature on the production of activated carbon from paulownia (*P. tomentose*) wood [20]. There is no reported research on the use of activated carbon obtained from paulownia wood for dye removal.

In our previous studies, [20] activated carbon with a high-surface area was prepared from paulownia (*P. tomentose*) wood by chemical activation with $ZnCl^2$ at different temperatures. In the present study, activated carbon thus produced was used for the removal of methylene blue (MB) from aqueous solutions. The effect of factors including pH, initial dye concentrations, contact times, temperatures and adsorbent doses on MB removal were investigated in a batch system. Kinetic models were used to identify the possible mechanisms of the adsorption process. The equilibrium data were analyzed by the Langmuir and Freundlich isotherm models. The thermodynamics of the adsorption process were studied, and the changes in Gibbs free energy and the enthalpy and the entropy of adsorption were also been determined; these are important parameters required for the design of any industrial adsorption system.

2. Experimental

2.1. Material and preparation of activated carbon

Paulownia wood used in this study as a raw material was obtained from the Çorum Black Sea region in Turkey. Prior to use, wood was air dried, ground in a high-speed rotary cutting mill, and screened to give the fraction of $0.6 < Dp < 1.8$ mm particle size for chemical activation with $ZnCl_2$. Elemental analyses of the wood and activated carbon were performed on a Carlo Erba Model EA 1108 elemental analyzer. The proximate and ultimate analyses of the paulownia wood and activated carbon are given in Table 1. The adsorbent was prepared from paulownia wood by chemical activation with $ZnCl_2$. The activation temperature and $ZnCl_2$/paulownia sawdust ratio (impregnation ratio) were selected as 400°C and 4/1, respectively. In the first step of activation, 80 grams of $ZnCl_2$ was dissolved in 200 mL of distilled water, and 20 g of the wood sawdust was mixed with the $ZnCl_2$ solution and stirred at approximately 80°C for 7 h. The mixture was then filtered and the remaining solid was dried at 110°C for approximately 12 h. In the second step, the impregnated sample was carbonized using a fixed-bed reactor. The 316 stainless steel reactor had a volume of 400 cm^3 (70 mm i.d.) and was externally heated by an electrical furnace in which the temperature was measured by a Ni–Cr thermocouple inside the bed. A more detailed description of the pyrolysis system and carbonization procedure has been reported elsewhere [20, 36]. The impregnated sample was heated to the final carbonization temperature (400°C) under 150 cm^3 min^{-1} nitrogen flow at a heating rate of 10°C min^{-1} and held for 1 h at this final temperature under N_2 gas flow. The resulting solid after carbonization was boiled at approximately 90°C with 100 mL of 1 N HCI solution for 30 min to leach out the activating agent. Subsequently, the activated sample was repeatedly washed with hot distilled water to remove residual chemicals until the pH of the solution reached 6.5, and the sample was washed with cold distilled water. Then, the activated carbon was dried at 110°C for 12 h and stored in a desiccator.

2.2. Characterization of textural properties of activated carbon

The pore structure characteristics of the activated carbon were determined by nitrogen adsorption at 77 K using an automatic adsorption instrument (Quantachrome, Autosorb-1C). Adsorption data were obtained over a range of relative pressure, P/P_o, from approximately 10^{-6} to 1.

The surface area, pore volume and pore size distribution of the activated carbon were determined by the Brunauer-Emmett-Teller (BET) method and the *t*-plot analysis software including with the instrument. The BET surface areas were assessed by applying relative pressures ranging from 0.01 to 0.15 [20]. The *t*-plot method was applied to micropore volume and mesopore surface area, and the mesopore volume was obtained by subtracting the micropore volume from the total pore volume. The pore size distribution of the activated carbon was obtained by applying the micromeritics density functional theory (DFT) method to nitrogen adsorption isotherms using the software supplied by Autosorb-1C.

2.3. Adsorption experiments

An adsorption technique for the treatment of MB dye-containing aqueous solution using activated carbon was investigated.

MB dye [C.I. = 52015, chemical formula, $C_{16}H_{18}ClN_3S.H^2O$, molecular weight, 337.85 g mol^{-1}, λ_{max} = 660 nm] was supplied by Merck. Dye stock solution (1,000 mg L^{-1}) was prepared by dissolving an accurately weighed quantity of the MB dye in double-distilled water. Experimental solutions of different concentrations were prepared by diluting the stock solution with suitable volumes of double-distilled water. Adsorption experiments were carried out by shaking a constant mass (0.1 g) of activated carbon with a constant volume (50 mL) of MB solution at initial dye concentration 400–1,000 mg L^{-1}. The flasks were agitated at a constant speed of 400 rpm in an isothermal shaker to reach solid-solution mixture equilibrium. The influence of pH (2–11), initial dye concentration (400–1,000 mg L^{-1}), contact time (1–25 h), temperature (24, 35 and 45°C), and adsorbent dose (0.05–0.3 g/50 mL) on the adsorption process was studied. Concentrations of the MB dyes were determined by measuring the absorbance at the characteristic wave length (660 nm) using a double-beam UV-vis spectrophotometer (Shimadzu UV 12001). The amount of dye adsorbed on the adsorbent surface was calculated as

$$q = \frac{(C_o - C_e)V}{m} \tag{1}$$

where q is the amount of dye the adsorbed onto the adsorbent (mg g^{-1}); C_o and C_e (mg L^{-1}) are the concentrations of dye at initial and equilibrium, respectively; V is the volume of the solution (L); and m is the mass of the adsorbent (g). The procedures followed in the kinetic experiments were similar to those used in the equilibrium experiments. Kinetic experiments were carried out at different temperatures (25 and 35°C). The aqueous samples were taken at preset time intervals, and concentrations of MB dye were similarly measured. The amount of adsorption at time t, was calculated as

$$q_t \frac{(C_o - C_t)V}{m} \tag{2}$$

where q_t is the amount of dye absorbed onto adsorbent (mg g^{-1}); C_o and C_t (mg L^{-1}) are the liquid-phase concentrations of dye at initial and any time t, respectively; V is the volume of the solution (L); and m is the mass of the activated carbon (g). The percentage removal of MB dye was calculated by using the following equation:

$$\text{Removal (\%)} = \frac{(C_o - C_e)}{C_o} \times 100 \tag{3}$$

where C_o and C_e (mg L^{-1}) are the initial and equilibrium dye concentrations, respectively. All the experiments were carried out in two replicates and the average values were used for further calculations.

2.4. Adsorption kinetics

Kinetic analysis can help to determine the mechanism of the adsorption process, whether controlled by chemical reaction or diffusive mass transfer. Thus, the most commonly used kinetic models including pseudo-first order, pseudo-second order and intraparticle diffusion were applied for the batch experiments [37, 38].

The pseudo-first order equation is expressed as follows [17, 39, 40]:

$$\ln(q_e - q_t) = \ln(q_e) - k_1 t \tag{4}$$

where q_e and q_t are the amounts of dye adsorbed (mg g^{-1}) at equilibrium and at time t (min), respectively, and k_1 is the rate constant for pseudo-first-order adsorption (min^{-1}). The k_1 values and q_e were calculated from the slope and intercept of the plots of $\ln(q_e - q_t)$ versus t for different temperatures, respectively (Fig. 7). The k_1 values, calculated q_e value and correlation coefficient are given in Table 3.

The pseudo-second-order equation is expressed as [6, 39, 41]:

$$\frac{t}{q_t} = \frac{1}{k_2 q_e^2} + \frac{1}{q_e} t \tag{5}$$

where q_e and q_t are amounts of dye adsorbed (mg g^{-1}) at equilibrium and time t (min), respectively, and k^2 is the rate constant of pseudo-second-order adsorption (g mg^{-1} min^{-1}). The plot of t/q_t against t at different temperatures is shown in Fig. 8. The values of the pseudo-second order model constants (q_e and k^2) were determined from the slope and intercept of these plots, respectively. The k^2 values, calculated q_e value and correlation coefficient are given in Table 3.

The intraparticle diffusion varying with the square root of time is given by [42]:

$$q_t = k_{id} t^{0.5} \tag{6}$$

where q_t is the amount (mg g^{-1}) adsorbed at a given time, t is the time (min) and k_{id} (mg g^{-1} $min^{-0.5}$) is the rate constant of intraparticle diffusion. The intraparticle diffusion rate constant was determined from the slope of the plot of q_t versus $t^{0.5}$ as

shown in Fig. 9. The k_{id} values, calculated q_e and correlation coefficients are given in Table 3.

2.5. Adsorption isotherms

The equilibrium relationship between adsorbents and adsorbates can be described by adsorption isotherms. Adsorption isotherms are basic requirements for the analysis and design of adsorption systems [6]. Langmuir and Freundlich models were chosen because they are simple and they give a good description of experimental behaviour across a large range of operating conditions. In general, the Langmuir equation is intended for a homogenous surface; a good fit of this equation reflects monolayer adsorption. On the other hand, a good fit with the Freundlich equation, which is suitable for a highly heterogeneous surface, most likely indicates multilayer adsorption [14]. In this study, the experimental data were applied to the Langmuir and Freundlich isotherm equations. The Langmuir isotherm equation is represented by the following equation [1, 6, 39, 41, 43]:

$$\frac{C_e}{q_e} = \frac{1}{Q_o b} + \frac{C_e}{Q_o} \tag{7}$$

where C_e is the dye concentration at equilibrium (mg L^{-1}), q_e is the adsorption capacity in equilibrium (mg g^{-1}), b is the Langmuir adsorption constant (L mg^{-1}) and Q^o signifies adsorption capacity (mg g^{-1}). Fig. 11 shows the Langmuir (C_e/q_e) versus (C_e) plots for the removal of MB dye at different temperatures. The linear form of the Freundlich isotherm equation is represented by the following equation [6, 11, 13, 14, 44]:

$$\ln(q_e) = \frac{1}{n}\ln(C_e) + \ln K_f \tag{8}$$

where q_e is the amount of dye adsorbed at equilibrium (mg g^{-1}), C_e is the equilibrium concentration of dye in the solution (mg L^{-1}), and k_f (L g^{-1}) and n are isotherm constants indicating the capacity and intensity of the adsorption, respectively. Fig. 12 shows the plots of $\ln(q_e)$ versus $\ln(C_e)$ at 25, 35 and 45°C adsorption temperatures. The values of k_f and n were calculated from the slope and intercept of the plot of $\ln(q_e)$ versus $\ln(C_e)$.

2.6. Estimation of thermodynamic parameters

Thermodynamic parameters were determined by analyzing Langmuir adsorption isotherms obtained at 25, 35 and 45°C. The changes in standard free energy (ΔG°), enthalpy (ΔH°) and entropy (ΔS°) of adsorption were calculated from the following equations [1, 38, 41–42]:

$$\Delta G° = RT \ln K_c \tag{9}$$

where R is the gas constant (8.314 J mol^{-1} K^{-1}), K_c is the equilibrium constant and T is temperature in K. The K_c value is calculated from the following equation:

$$K_c = \frac{C_{Ae}}{C_{Se}} \tag{10}$$

where C_{Ae} and C_{Se} are the equilibrium concentrations of the dyestuff on activated carbon (mgL^{-1}) and in the solution (mgL^{-1}), respectively. Standard enthalpy (ΔH°) and entropy (ΔS°) of the adsorption can be estimated from the van't Hoff equation:

$$\ln K_c = \frac{\Delta S^\circ}{R} - \frac{\Delta H^\circ}{RT} \tag{11}$$

The values of ΔH° and ΔS° were calculated from the slope and intercept of the van't Hoff plot of $\ln(K_c)$ versus 1/T (Fig. 13) and are listed in Table 5.

3. Results and discussion

3.1. Material and characterization of textural properties of activated carbon

The proximate and ultimate analyses of the raw material and activated carbon are presented in Table 1. The high volatile matter and low ash content of a biomass resource make it a good starting material for preparing activated carbon [24]. As shown in Table 1, paulownia wood has low ash and high volatile matter contents. The high concentration of volatiles associated with paulownia wood is ideal for creating highly porous structures within the activated carbon matrix. Activated carbon contains high ratios of mass transfer voids [27]. Because the thermal treatment removes the moisture and the volatile matter contents of the wood, the activated carbon shows different properties from the paulownia wood. The important differences are mainly in physical-chemical properties such as composition, elemental analysis, and ash content when the composition of the activated carbon is compared with that of the paulownia wood: the carbon level increases and the oxygen and hydrogen levels decrease. These changes are due to the liberation of volatile compounds during the carbonization and activation process. The H/C molar ratio was lower for the paulownia wood compared with the activated carbon. This decrease from 1.64 to 0.38 indicates a higher degree of aromaticity of the activated carbon. A similar trend has also been reported in the literature [45, 46]. Fig. 1 shows the adsorption-desorption isotherm of the activated carbon prepared from paulownia wood by chemical activation with $ZnCl_2$. It is clear that the carbon activated by $ZnCl_2$ had higher adsorption capacity (per unit mass). This higher capacity is due to the larger volumes of micropore and mesopore in the structure of activated carbon. As shown in Fig. 1, at low relative pressure, a rapid increase in the adsorption-desorption isotherm was observed when relative pressure was increased. This increase was followed by a nearly horizontal plateau at higher relative pressure, indicating a type I isotherm based on the classification of Brunauer, Deming, Deming and Teller (BDDT); small closed hysteresis loops indicates the existence of both micro and mesopores. The type I isotherm is associated with microporous structured material. The major uptake that occurred at low relative pressure indicated the formation of highly porous materials with a narrow pore size distribution as shown in Fig. 2. The pore size distribution of activated carbon is an important factor

Table 1
Proximate and ultimate analyses of paulownia wood and activated carbon (prepared at impregnation ratio of 4 and carbonization temperature of 400°C) [20]

Analysis	Wood (wt%)	Activated carbon (wt%)	ASTM test standard
Proximate			
Moisture	6.50	3.20	D 2016-74
Ash	1.06	2.65	D 1102-84
Volatile matter	71.80	13.80	E 987-82
Fixed carbon[2]	20.64	80.35	
Ultimate			
Carbon	44.73	71.36	
Hydrogen	6.12	2.25	
Oxygen[1]	48.28	25.93	
Nitrogen	0.87	0.46	
H/C molar ratio	1.64	0.38	
O/C molar ratio	0.81	0.72	
Calorific value (MJ/kg)	20.6	25.3	D 3286
Empirical formula	$CH^{1.64}O^{0.81}N^{0.02}$	$CH^{0.38}O^{0.27}N^{0.005}$	

[1,2] By difference

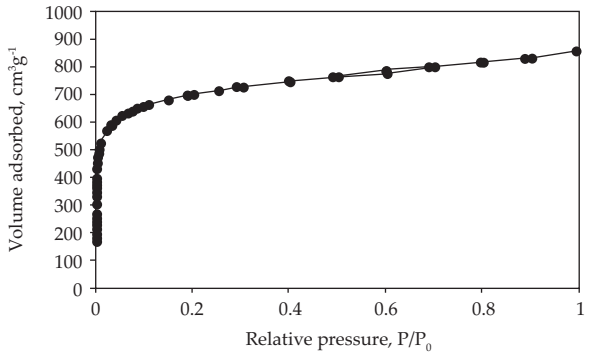

Fig. 1. Nitrogen adsorption-desorption isotherm for activated carbon.

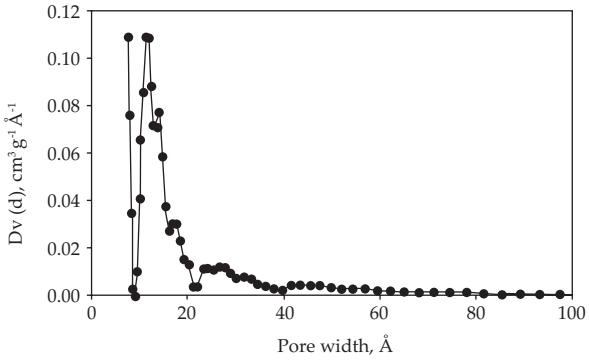

Fig. 2. Pore size distribution of the activated carbon.

for application in specific process operations. As shown in Fig. 2, it appears that the activated carbon was dominantly microporous.

Table 2 shows the pore properties of carbon including S_{BET}, S_{mi}, S_{me}, V_t, V_{mi}, V_{me} and average pore diameter (Dp). The experimental results show that the activated carbon included micropores and mesopores. The percentage of micropore and mesopore surface areas were 63.1%, and 36.9%, respectively. S^{BET} and total pore volume were found to be 2,736 $m^2\ g^{-1}$ and 1.387 $cm^3\ g^{-1}$, respectively. Activated carbon obtained from wood had a high surface area and pore volume comparable with commercially produced activated carbons with a typical surface area range from 500 to 2,000 $m^2\ g^{-1}$ [47].

3.2. Adsorption experiments

3.2.1. Effect of initial pH

The efficiency of adsorption is dependent on the solution pH. The initial pH of dye solution is one of the important factors controlling the adsorption of dye molecules onto suspended particles by affecting the surface charge of the adsorbents as well as the degree of ionization of adsorbate [14, 44]. The MB, being a cationic dye, gives positively charged ions when dissolved in water. The acidic condition produces more H^+ ions in the system. The percentage removal of the MB dye as a function of pH is shown in Fig. 3. The removal of MB by activated carbon was found to increase with the pH of the dye solution.

In the acidic region, the surface of the activated carbon gathers positive charges by adsorbing H^+ ions which prevent the adsorption of MB dye ions onto adsorbent surface due to electrostatic repulsion and the competition between H^+ ion and MB for the adsorption sites [14, 44]. A further increase in dye adsorption between pH = 2 and 7 was insignificant. However, with the increasing solution pH values, the adsorption of MB on activated carbon tends to increase, which can be explained by the electrostatic interaction of the cationic dye species with the negatively charged adsorption sites. The electrostatic force of attraction increases with increasing negative surface charge of the activated carbon [14, 44].

Table 2
Surface area and porosity of the activated carbon

S_{BET} ($m^2\ g^{-1}$)	S_{mi} ($m^2\ g^{-1}$)	S_{mi} (%)	S_{me} ($m^2\ g^{-1}$)	S_{me} (%)	V_t ($cm^3\ g^{-1}$)	V_{mi} ($cm^3\ g^{-1}$)	V_{mi} (%)	V_{me} ($cm^3\ g^{-1}$)	V_{me} (%)	D_p (nm)
2736	1727	63.1	1009	36.9	1.387	0.690	49.7	0.697	50.3	2.17

S_{BET}: BET surface area, S_{mi}: micropore surface area, S_{me}: mesopore surface area, V_t: total pore volume, V_{mi}: micropore volume, V_{me}: mesopore volume, D_p: particle size, S_{mi} (%) = (S_{mi}/S_{BET}).100, S_{me} (%) = (S_{me}/S_{BET}).100, V_{mi} (%) = (V_{mi}/V_t).100, V_{me} (%) = (V_{me}/V_t).100.

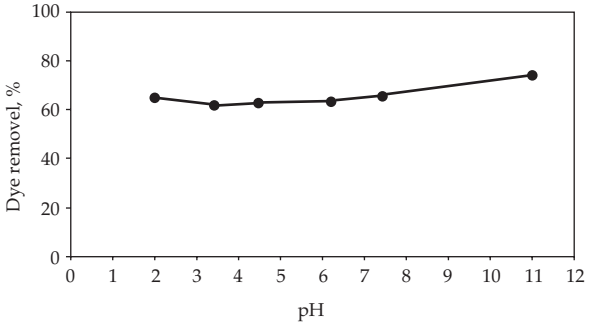

Fig. 3. Effect of the initial solution pH on MB removal by activated carbon (T = 25°C, *Co* = 1000 mg L^{-1}, adsorbent dose = 0.1 g/0.05 L, equilibrium time = 24 h).

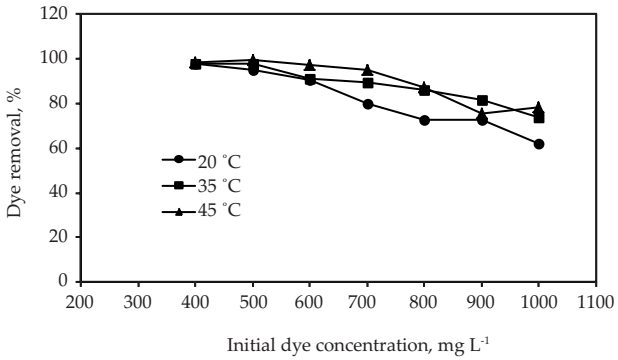

Fig. 4. Effect of the initial dye concentration on methylene blue removal by activated carbon at different temperatures (adsorbent dose = 0.1 g/0.05 L, equilibrium time = 24 h).

These interactions facilitate higher adsorption capacity. The dye removal percentage increased with significant enhancement in the adsorption process as the pH increased from 7 to 11. A similar trend was observed in the effect of pH on the adsorption of MB onto activated bituminous coal in a previous study [14]. The percentage of dye removal increased from 65% to 75% with increasing pH from 2 to 11. An increase in the pH value caused only a slight increase in the removal efficiency. This was negligible. Similar results have been reported for adsorption of MB onto dehydrated wheat bran carbon [44]. Therefore, further experiments were conducted without adjusting the initial solution pH.

3.2.2. The effect of initial dye concentration and contact time at different temperatures

The percentage removal of MB on both of the activated carbons at different temperatures (25, 35 and 45°C) and different initial dye concentrations (400–1,000 mg L^{-1}) are shown in Fig. 4. In all cases, the percentage removal of dye decreased with increasing initial dye concentration. The uptake is almost 100% at low dye concentration for all temperatures. At higher initial dye concentrations, lower adsorption yields were observed. This lower yield may be due to the surface saturating with dye molecules and the formation of a monolayer by the adsorbate on the activated carbon surface [48]. The percentage of dye removal decreased from 100% to 62–79% as the initial concentration of dye was increased from 400 to 1,000 mg L^{-1}. Furthermore, the uptake of dye increased with temperature when the temperature was raised from 25 to 45°C. The removal percentages of dye increased from 62% to 79% for an initial dye concentration of 1,000 mg L^{-1}. The uptake of MB increasing with temperature indicated that the adsorption process was endothermic. A similar result has been reported in the literature for the removal of MB by different activated carbons [15]. Fig. 5 shows the effect of contact time on the percentage of MB removed at 25 and 35°C. The uptake of dye was rapid initially and slowed as time proceeded. The percentage of dye removed was observed to increase with increasing contact time and temperature. Equilibrium was practically attained after 24 h.

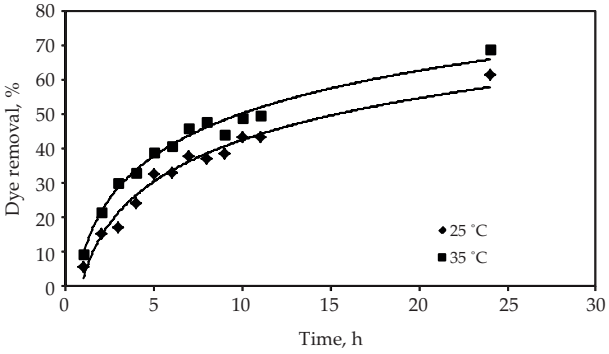

Fig. 5. Effect of contact time on methylene blue removal by activated carbon at different temperatures (*Co* = 1000 mg L^{-1}, adsorbent dose = 0.5 g/0.25 L).

3.2.3. Effect of adsorbent dose

The effect of adsorbent dosage on the removal of MB by activated carbon is shown in Fig. 6. Dye removal increased with adsorbent dosage up to a certain limit and then

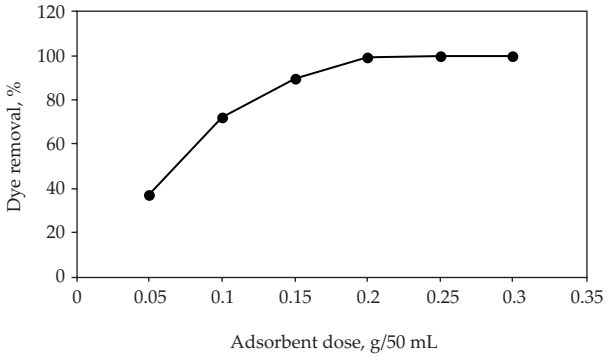

Fig. 6. Effect of adsorbent dose on methylene blue removal by activated carbon (T = 25°C, *Co* = 1000 mg L^{-1}, equilibrium time = 24 h).

remained almost constant as more adsorbent was added. The percent removal of dye varied from 35% to 100% with an increase in adsorbent dosage from 0.05 to 0.2 g, and further addition of adsorbent did not affect the adsorption process. It is understood that the number of available adsorption sites and the surface area both increase by increasing the activated carbon dose. A similar trend has been reported for adsorption of MB and colored effluent by different activated carbons [44, 48].

3.3. Kinetic analysis

In this study, the pseudo-first-order, pseudo-second-order and intraparticle diffusion models were used to obtain rate constants, equilibrium adsorption capacities, and adsorption mechanisms at different temperatures. These models are shown in Figs. 7, 8 and 9 for the effects of temperature on adsorption. A comparison of these kinetics results is given in Table 3. The correlation coefficient R^2 for the pseudo-second-order adsorption model was large (>98%), and its calculated equilibrium adsorption capacity, $q_{e,cal}$ was consistent with experimental data, $q_{e,exp}$. In addition, the rate constant, k_2, increased as the temperature increased from 25 to 35°C. These facts suggest that the pseudo-second-order adsorption mechanism is predominant, and that the overall rate of the MB adsorption process appears to be controlled by the rate of the chemisorption process. Similar results have been observed in the adsorption of MB onto different adsorbents [6, 39, 49].

3.4. Adsorption isotherms

Fig. 10 shows the plots of adsorption isotherms, q_e versus C_e for the MB-activated carbon system at different temperatures. Figure. 10 shows that, with an increase in temperature, the adsorptivity of MB increased. It was found that q_e increased sharply with C_e at lower dye concentrations and then gradually plateaued. The plateau of the adsorption isotherm shows the adsorption capacity of an adsorbent. The capacity of activated carbon for MB can be determined by measuring equilibrium isotherms,

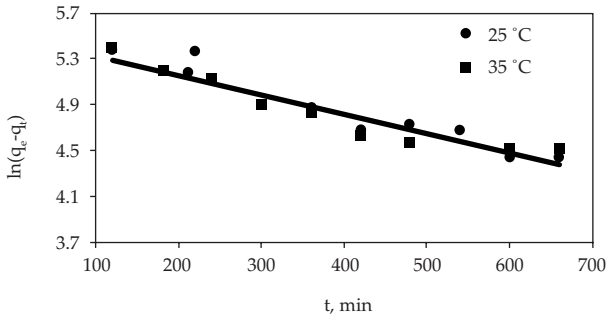

Fig. 7. The pseudo-first-order adsorption kinetics of MB at different temperatures (C_o = 1000 mg L^{-1}, adsorbent dose = 0.1 g/0.05 L).

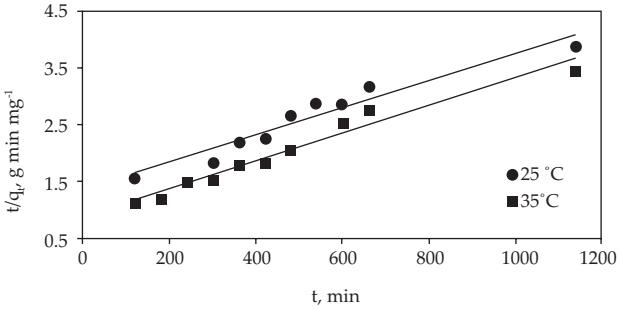

Fig. 8. The pseudo-second-order adsorption kinetics of MB at different temperatures (C_o = 1000 mg L^{-1}, adsorbent dose = 0.1 g/0.05 L).

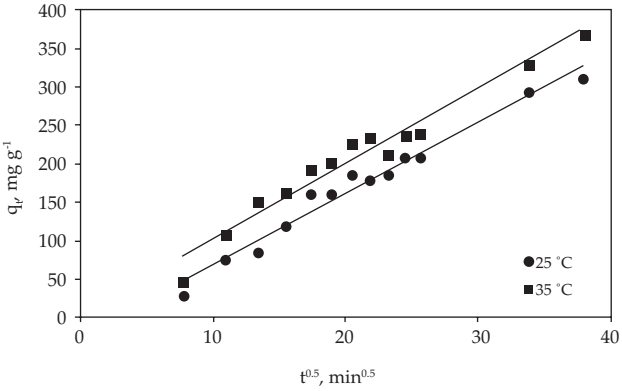

Fig. 9. Intraparticle diffusion plots of MB onto activated carbon at different temperatures (adsorbent dose = 0.1 g/0.05 L).

and the adsorption experimental data were applied to Langmuir and Freundlich isotherm equations. The values of the Langmuir and Freundlich parameters were obtained, respectively, from Figs. 11 and 12. The Langmuir and Freundlich constants are very useful parameters for predicting adsorption capacities. The constant parameters and correlation coefficient (R^2) are given in Table 4. As shown in Table 4, the Langmuir isotherm model fit the experimental data well with high correlation coefficients at all temperatures. The monolayer adsorption capacity, Q_o, increased

Table 3
Comparison of the kinetic constants for pseudo-first-order, pseudo-second-order and intra-particle diffusion

Temperature (°C)	Pseudo-first-order				Pseudo-second-order			Intra-particle diffusion		
	$q_{e,exp}$ (mg g^{-1})	$q_{e,cal}$ (mg g^{-1})	k^1 (min^{-1})	R^2	$q_{e,cal}$ (mg g^{-1})	k^2 (10^{-5}) (g mg^{-1} min^{-1})	R^2	q_e (mg g^{-1})	k_{int} (g mg^{-1} min$^{-0.5}$)	R^2
25	293.50	241.51	0.0017	0.930	322.58	0.88	0.960	310.27	9.87	0.9721
35	329.25	241.65	0.0017	0.917	333.33	1.30	0.987	370.13	9.85	0.9441

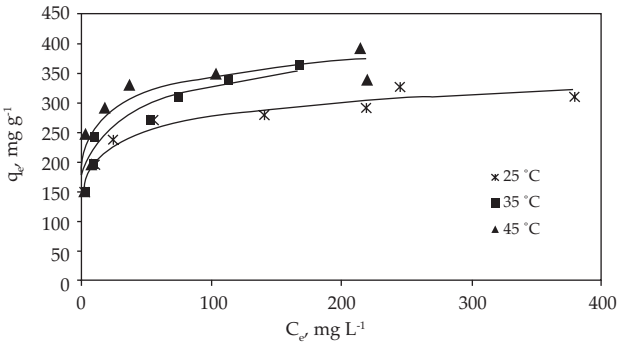

Fig. 10. Equilibrium adsorption isotherms of MB onto activated carbon at different temperatures (adsorbent dose = 0.1 g/0.05 L).

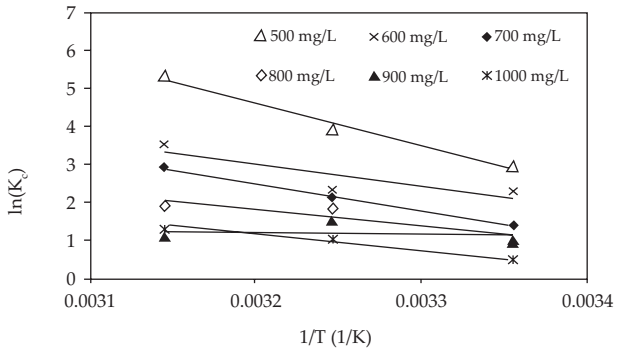

Fig. 13. ln *Kc* versus 1/T for adsorption of MB at temperature of 298, 308 and 318 K.

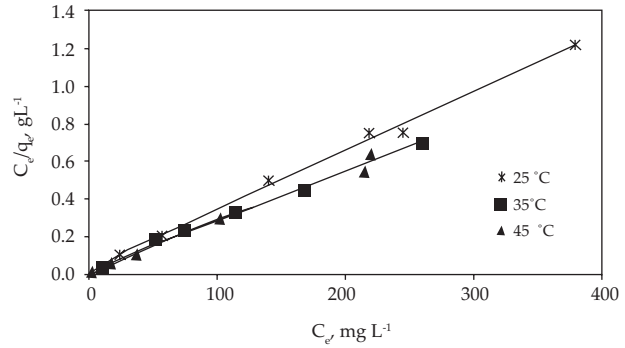

Fig. 11. Langmuir adsorption isotherms for MB onto activated carbon at different temperatures (adsorbent dose = 0.1 g/0.05 L).

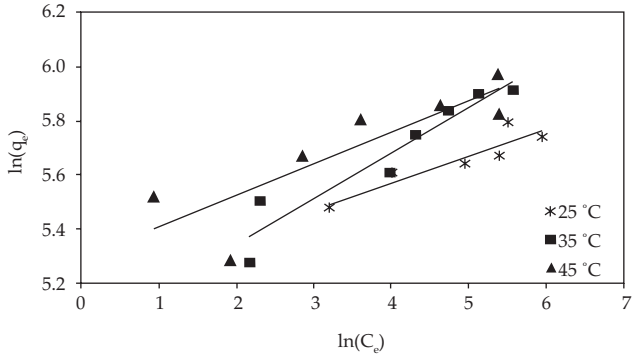

Fig. 12. Freundlich adsorption isotherms for MB onto activated carbon at different temperatures (adsorbent dose = 0.1 g/0.05 L).

with temperature over the range of 25–45°C. The maximum adsorption capacity for MB onto activated carbon at 45°C was estimated to be 384.61 mg g^{-1}.

Table 5 compares the maximum monolayer adsorption capacities of some dyes on various adsorbents. The activated carbon described in this study has a very large adsorption capacity compared with many of the other reported adsorbents.

3.5. Estimation of thermodynamic parameters

Values of the thermodynamic parameters for the adsorption of MB onto activated carbon are given in Table 6. The positive value of ΔH° indicates that the adsorption of MB onto activated carbon is an endothermic process. The positive value of ΔS° suggests good affinity of MB towards the activated carbon, with some structural changes occurring in the MB and activated carbon. Randomness increases at the solid/solution interface during chemisorption [11]. The negative value of the free energy change ΔG° suggests that the adsorption process is spontaneous, and the affinity of the adsorbent for MB is indicated by the positive value of the entropy change. As shown in Table 5, the decreasing value of ΔG° with increasing temperature indicates a greater driving force at higher temperatures, resulting in more adsorption capacity at higher temperatures. A similar trend has been reported for MB adsorption onto a waste apricot adsorbent [11].

4. Conclusion

An activated carbon prepared from paulownia wood by chemical activation with $ZnCL_2$ has been used succesfully for the removal of the MB from aqueous solution. The produced

Table 4
Langmuir and Freundlich adsorption isotherms parameters for activated carbon

	Langmuir isotherm			Freundlich isotherm		
Temperature (°C)	Q_o (mg g^{-1})	b (L mg^{-1})	R^2	k	n	R^2
25	322.58	0.085	0.9944	176.21	10.05	0.8467
35	370.37	0.237	0.9907	148.78	5.90	0.9164
45	384.61	0.080	0.9962	198.88	8.56	0.7281

Table 5
Comparison of maximum monolayer adsorption capacity of some dyes on various adsorbents

Adsorbent	Dye	Capacity (mg/g)	Refs.
Pine wood	Malachite green	42.63	[11]
Pitch-pine sawdust	Bismarck brown	27.78	[12]
Oak wood sawdust	Methylene blue	29.94	[12]
Cherry wood sawdust	Methylene blue	39.84	[12]
Walnut sawdust	Methylene blue	59.17	[12]
Rubber wood	Malachite green	124.47–144.52	[17]
Mansonia wood sawdust	Methylene blue	33.44	[31]
Aleppo pine sawdust	Astrazon yellow	81.80	[32]
Mahogany sawdust	Acid dyes	138.80	[50]
Pine sawdust	Malachite green	370.37	[51]
Wood apple	Methylene blue	35.10	[52]
Paulownia wood sawdust	Methylene blue	384.61	This study

Table 6
Values of thermodynamic parameters for the adsorption of MB onto activated carbon

C_o (mg L^{-1})	ΔH° (kJ mol^{-1})	ΔS° (kJ mol^{-1} K^{-1})	$^{-}$ΔG° (kJ mol^{-1})		
			298 K	308 K	318 K
500	91.06	0.329	7.35	9.98	13.97
600	48.19	0.179	5.65	5.97	9.30
700	59.46	0.210	3.43	5.47	7.65
800	37.43	0.134	2.42	4.61	5.08
900	36.15	0.129	2.44	3.78	2.99
1,000	31.78	0.111	1.22	2.68	3.42

activated carbon migh be a low cost alternative compared to the use of commercial activated carbons and other adsorbents.

It was found that the high volatile matter and low ash contents of paulownia wood make it a good starting raw material for preparing activated carbon. Textural characteristics of activated carbon were found to be strongly dependent on the impregnation ratio and final chemical activation temperature. It may be concluded that $ZnCL^2$ is more effective as a chemical reagent in terms of high surface area, porosity development and surface morphology of the activated carbon. Depending on the chemical activation conditions, the produced activated carbon exhibited well developed porosity and narrow size distribution that was essentially microporous. The activated carbon was evaluated as a possible adsorbent for the removal of MB from aqueous solutions due to its high surface area, pore volume and porosity.

The results showed that the uptake of MB increased with increasing contact time, temperature and adsorbent dosage but decreased with initial dye concentration. The pH value did not affect the adsorption process considerably. The rate of adsorption was found to fit pseudo-second-order

kinetics well. The negative value of ΔG° confirmed the spontaneous nature of the adsorption process. The positive value of ΔS° showed increased randomness at the solid-liquid interface during adsorption and the positive value of ΔH° showed that the adsorption process was endothermic.

References

[1] S. Senthilkumaar, P. Kalaamani, C.V. Subburaam, Liquid phase adsorption of crystal violet onto activated carbons derived from male flowers of coconut tree, J. Hazard. Mater., 136 (2006) 800–808.

[2] L. Yu, Q. Zhong, Preparation of adsorbents made from sewage sludges for adsorption of organic materials from wastewater, J. Hazard. Mater., 137 (2006) 359–366.

[3] A.S. Özcan, B. Erdem, A. Özcan, Adsorption of acid blue 193 from aqueous solutions onto Na-bentonite and DTMA-bentonite, J. Colloid Interface Sci., 280 (2004) 44–54.

[4] Z. Aksu, I.A. Isoglu, Use of agricultural waste sugar beet pulp for the removal of gemazol turquoise blue-G reactive dye from aqueous solution, J. Hazard. Mater., 137 (2006) 418–430.

[5] I.D. Mall, V.C. Srivastava, N.K. Agarwal, I.M. Mishra, Removal of congo red from aqueous solution by bagasse fly ash and activated carbon: Kinetic study and equilibrium isotherm analyses, Chemosphere, 61 (2005) 492–501.

[6] B.H. Hameed, A.L. Ahmad, K.N.A. Latiff, Adsorption of basic dye (methylene blue) onto activated carbon prepared from rattan sawdust, Dyes Pigm.,75 (2007) 143–149.

[7] W.Y. Abu-El-Shar, S.H. Gharaibeh, S. Mahmoud, Removal of dyes from aqueous solutions using low-cost sorbents made of solid residues from olive-mill wastes (JEFT) and solid residues from refined Jordanian oil shale, Environ. Geology, 39 (2000) 1090–1094.

[8] E.N. El Qada, S.J. Allen, G.M. Walker, Adsorption of basic dyes from aqueous solution onto activated carbons, Chem. Eng. J., 135 (2008) 174–184.

[9] T.C. Chandra, M.M. Mirna, Y. Sudaryanto, S. Ismadji, Adsorption of basic dye onto activated carbon prepared from durian shell: Studies of adsorption equilibrium and kinetics, Chem. Eng. J., 127 (2007) 121–129.

[10] F.C. Wu, R.L. Tseng, C.C. Hu, Comparisons of pore properties and adsorption performance of KOH-activated and steam-activated carbons, Micropor. Mesopor. Mater., 80 (2005) 95–106.

[11] H. Zhang, Y. Tang, X. Liu, Z. Ke, X. Su, D. Cai, X. Wang, Y. Liu, Q. Huang, Z. Yu, Improved adsorptive capacity of pine wood decayed by fungi *Poria cocus* for removal of malachite green from aqueous solutions, Desalination, 274 (2011) 97–104.

[12] F. Ferrero, Dye removal by low cost adsorbents: Hazelnut shells in comparison with wood sawdust, J. Hazard. Mater., 142 (2007) 144–152.

[13] V.S. Mane, I.D. Mall, V.C. Srivastava, Kinetic and equilibrium isotherm studies for the adsorptive removal of brilliant green dye from aqueous solution by rice husk ash, J. Environ. Manage., 84 (2007) 390–400.

[14] E.N. El Qada, S.J. Allen, G.M. Walker, Adsorption of methylene blue onto activated carbon produced from steam activated bituminous coal: A study of equilibrium adsorption isotherm, Chem. Eng. J., 124 (2006) 103–110.

[15] C.A. Başar, Applicability of the various adsorption models of three dyes adsorption onto activated carbon prepared waste apricot, J. Hazard. Mater., 135 (2006) 232–241.

[16] F.K. Yuen, B.H. Hameed, Recent developments in the preparation and regeneration of activated carbons by microwaves, Adv. Colloid Interface Sci., 149 (2009) 19–27.

[17] S. Rajgopal, T. Karthikeyan, B.G.P. Kumar, L.S. Miranda, Utilization of fluidized bed reactor for the production of adsorbents in removal of malachite green, Chem. Eng. J., 116 (2006) 211–217.

[18] F.C. Wu, R.L. Tseng, Preparation of highly porous carbon from fir wood by KOH etching and CO_2 gasification for adsorption of dyes and phenols from water, J. Colloid Interface Sci., 294 (2006) 21–30.

[19] Ç. Şentorun-Shalaby, M.G. Uçak-Astarlioglu, L. Artok, Ç. Sarıcı, Preparation and characterization of activated carbons by one-step steam pyrolysis/activation from apricot stones, Micropor. Mesopor. Mater., 88 (2006) 126–134.

[20] S. Yorgun, N. Vural, H. Demiral, Preparation of high-surface area activated carbons from paulownia wood by $ZnCl_2$ activation, Micropor. Mesopor. Mater., 122 (2009) 189–194.

[21] J. Hayashi, N. Yamamoto, T. Horikawa, K. Muroyama, V.G. Gomes, Preparation and characterisation of high-specific-surface-area activated carbon from K_2CO_3-treated waste polyurethane, J. Colloid Interface Sci., 281 (2005) 437–443.

[22] J.M. Dias, M.C.M. Alvim-Ferraz, M.F. Almeida, J. Rivera-Utrilla, M. Sánchez-Polo, Waste materials for activated carbon preparation and its use in aqueous-phase treatment: A review, J. Environ. Manage., 85 (2007) 833–846.

[23] K. Mohanty, D. Das, M.N. Biswas, Adsorption of phenol from aqueous solutions using activated carbon prepared from Tectona grandis sawdust by $ZnCl_2$ activation, Chem. Eng. J., 115 (2005) 121–131.

[24] A.C. Lua, F.Y. Lau, J. Guo, Influence of pyrolysis conditions on pore development of oil-palm-shell activated carbons, J. Anal. Appl. Pyrol., 76 (2006) 96–102.

[25] H. Deng, G. Li, H. Yang, J. Tang, J. Tang, Preparation of activated carbon from cotton stalk by microwave assisted KOH and K_2CO_3 activation, Chem. Eng. J., 163 (2010) 373–381.

[26] M.A. Díaz-Díez, V. Gómez-Serrano, C.F. González, E.M. Cuerda-Correa, A. Macías-García, Porous texture of activated carbons prepared by phosphoric acid activation of woods, Appl. Surf. Sci., 238 (2004) 309–313.

[27] F.C. Wu, R.L. Tseng, R.S. Juang, Preparation of highly microporous carbons from fir wood by KOH activation for adsorption of dyes and phenols from water, Sep. Purif. Technol., 47 (2005) 10–19.

[28] B.G.P. Kumar, L.R. Miranda, M. Velan, Adsorption of bismark brown dye on activated carbons prepared from rubber wood sawdust (*Hevea brasiliensis*) using different activation methods, J. Hazard. Mater., 126 (2005) 63–70.

[29] A. Azizi, M.R.A. Moghaddam, M. Arami, Application of wood waste for removal of reactive blue 19 from aqueous solutions: Optimization through response surface methodology, Environ. Eng. Manage J., 11 (2012) 795–804.

[30] R. Ansari, M.S. Tehrani, A. Mohammad-Khah, Highly efficiently dye removal from aqueous solutions using simple chemical modification of wood sawdust, J. Wood. Chem. Technol., 32 (2012) 198–209.

[31] A.E. Ofomaja, Equilibrium sorption of methylene blue using mansonia wood sawdust as biosorbent, Desalin. Water Treat., 3 (2009) 1–10.

[32] N. Ouazene, M.N. Sahmoune, Equilibrium and kinetic modelling of astrazon yellow adsorption by sawdust: Effect of important parameters, Int. J. Chem. React. Eng. 8, Article Number, A151 (2010).

[33] Z.H. Zhu, C.J. Chao, X.Y. Lu, Y.G. Xiong, *Paulownia* in China: Cultivation and Utilization, Asian Network of Biological Sciences, Singapore and International Development Research Center, Canada 1986, pp. 1–65.

[34] B.A. Bergmann, Five years of paulownia field trials in North Carolina, New Forests, 25 (2003) 185–199.

[35] B.A. Bergmann, Propagation method influences first year field survival and growth of paulownia, New Forests, 16 (1998) 251–264.

[36] S. Yorgun, Y.E. Şimşek, Fixed-bed pyrolysis of *miscanthus x giganteus*: product yields and bio-oil characterization, Energy Sources, 25 (2003) 779–790.

[37] B. Kayranli, Adsorption of textile dyes onto iron based waterworks sludge from aqueous solution: isotherm, kinetic and thermodynamic study, Chem. Eng. J., 173 (2011) 782–791.

[38] Y. Önal, C. Akmil-Başar, D. Eren, Ç. Sarıcı-Özdemir, T. Depci, Adsorption kinetics of malachite green onto activated carbon prepared from Tunçbilek lignite, J. Hazard. Mater., 128 (2006) 150–157.

[39] B.H. Hameed, A.T.M. Din, A.L. Ahmad, Adsorption of methylene blue onto bamboo-based activated carbon: Kinetics and equilibrium studies, J. Hazard. Mater., 141 (2007) 819–825.

[40] S. Wang, L. Li, H. Wu, Z.H. Zhu, Unburned carbon as low-cost adsorbent for treatment of methylene blue-containing waste water, J. Colloid Interface Sci., 292 (2005) 336–343.
[41] Y. Önal, C.A. Akmil-Başar, Ç. Sarıcı-Özdemir, Investigation kinetics mechanisms of adsorption malachite green onto activated carbon, J. Hazard. Mater., 146 (2007) 194–203.
[42] T. Karthikeyan, S. Rajgopal, L.R. Miranda, Chromium (VI) adsorption from aqueous solution by hevea brasilinesis sawdust activated carbon, J. Hazard. Mater., 124 (2005) 192–199.
[43] S. Senthilkumaar, P. Kalaamani, K. Porkodi, P.R. Varadarajan, C.V. Subburaam, Adsorption of dissolved reactive red dye from aqueous phase onto activated carbon prepared from agricultural waste, Bioresour. Technol., 97 (2006) 1618–1625.
[44] A. Özer, G. Dursun, Removal of methylene blue from aqueous solution by dehydrated wheat bran carbon, J. Hazard. Mater., 146 (2007) 262–269.
[45] C. Namasivayam, D. Sangeetha, Recycling of agricultural solid waste, coir pith: Removal of anions, heavy metals, organics and dyes from water by adsorption onto $ZnCI^2$ activated coir pith carbon, J. Hazard. Mater., 135 (2006) 449–452.
[46] F.F. Avelar, M.L. Bianchi, M. Gonçalves, E.G. Mota, The use of piassava fibers (Attalea funifera) in the preparation of activated carbon, Bioresour. Technol., 101 (2010) 4639–4645.
[47] P.T. Williams, A.R. Reed, Development of activated carbon pore structure via physical and chemical activation of biomass fibre waste, Biomass Bioenergy, 30 (2006) 144–152.
[48] M.M. Karim, A.K. Das, S.H. Lee, Treatment of colored effluent of the textile industry in Bangladesh using zinc chloride treated indigenous activated carbons, Analytica Chimica Acta, 576 (2006) 37–42.
[49] Y. Önal, Kinetics of adsorption of dyes from aqueous solution using activated carbon prepared from waste apricot, J. Hazard. Mater., 137 (2006) 1719–1728.
[50] P.K. Malik, Use of activated carbons prepared from sawdust and rice-husk for adsorption of acid dyes: a case study of acid yellow 36, Dyes Pigm., 56 (2003) 239–249.
[51] C. Akmil-Başar, Y. Önal, T. Kılıçer, D. Eren, Adsorptions of high concentration malachite green by two activated carbons having different porous structures, J. Hazard. Mater., 127 (2005) 73–80.
[52] N. Bhadusha, T. Ananthabaskaran, Adsorptive removal of methylene blue onto $ZnCl_2$ activated carbon from wood apple outer shell: Kinetics and equilibrium studies, E-Jour. Chem., 8 (2011) 1696–1707.